Article

Underground MV Network Failures' Waveform Characteristics—An Investigation

Miguel Louro [1],* and Luís Ferreira [2]

1   EDP Distribuição, 1050-044 Lisbon, Portugal
2   Department of Electrical Engineering and Computers, Instituto Superior Técnico, 1049-001 Lisbon, Portugal; lmf@tecnico.ulisboa.pt
*   Correspondence: miguel.louro@edp.pt

Abstract: The authors seek to investigate the characteristics of outage-causing faults that can be observed in a short time frame after their occurrence: waveform of the voltages and currents. The aim is to identify which characteristics can be used to estimate the failure type immediately after its occurrence. This paper lays the groundwork to determine which features display a stronger relation to four failure types with the aim of using this information in a later work, not presented in this paper, aimed at designing a reliable failure type estimator from readily available data. This paper focuses on the most common failures of the underground cable MV networks in Portugal: cable insulation; cable joint; secondary substation busbar; and excavation-motivated failures. A set of 206 waveform records of real underground MV network failures was available for analysis. After investigating the waveforms, the authors identified seven waveform characteristics which can be used for failure type estimation. Fault type characteristics can be used to distinguish secondary substation failures from the remaining failure types. Fault evolution does not yield relevant information. Fault self-extinction phenomenon was not observed in excavation-caused failures. There are differences for self-extinction characteristics between secondary substation busbar failures and the cable insulation and joint failures. Fault inception instant and arc voltage are two characteristics which are shown to have a promising merit to the identification process of failure types. Finally, fault intra-cycle repetitive extinction results have been found to be very similar for cable insulation failures and joint failures, but otherwise different regarding the remaining failure types.

Keywords: waveform; power distribution faults; underground network failures; failure estimation

1. Introduction

Electrical utilities are under constant regulatory pressure to reduce the number and duration of outages experienced by their clients. Presently, various fault location strategies, ranging from impedance-based methods [1–5], to simple trial and error methods, are used to achieve those goals. However, fault location can only supply information concerning an approximate fault area. Then, it is up to the field crew to find the failed element, typically by visual inspection of the corresponding overhead networks or, if in an underground network, by using specific equipment to locate the failure. If the field crew had some reliable information regarding the type of failure that caused the outage, it would result in a lower fault location and repair time. Additionally, it is very important to find the causes of non-persistent faults. For non-persistent faults, an automatic reclosure eliminates the fault, but not necessarily the cause of the fault. As time passes, the underlying cause of the fault still holds, and the fault evolves into a permanent fault, and causes an outage. A reliable estimation of the failure type is expected to increase the success rate and resource efficiency of locating these faults.

This paper is part of an ongoing effort to achieve a reliable failure type estimation based on various indirect observations. There is another paper being proposed by the

authors which assesses the relationship between failures and ambient observations: time; weekday; loading conditions; substation historical failure rate; precipitation; dew point; and ambient temperature. This paper has a different purpose: to contribute to the knowledge required to achieve a failure type estimator by investigation of the waveform characteristics of typical failures occurring in underground networks. The failure type estimator design is the subject of ongoing investigation and will not be presented in this paper. This type of approach has already been carried out in other fields such as [6]. Other authors have also focused on the conditions that lead to faults appearing in the power system [7].

The most typical failures in the Portuguese underground cable network are: cable insulation failure; cable joint failure; secondary substation busbar failure; excavation-caused failures (external aggressions).

A large number of waveform data concerning real failures in the Portuguese underground MV network was available to the authors. Over 200 events for the four foregoing failure types were available. This data is extensively used in the analysis. However, there may be some design options of the networks that influence the results; therefore, a small description of the MV underground networks in Portugal is provided. The underground MV network, under normal operation, presents a single point neutral connection to ground, and an impedance is placed between the neutral and the ground. Furthermore, the network cables (mostly three single core cables) are placed underground directly in the soil, no piping is used. Finally, the joints are also placed directly in the soil, no housing or access manhole exist.

A previous investigation on the waveform characteristics of failures types is provided in Reference [8], no further references addressing this subject with the detail of [8] were identified. That reference assesses several waveform data characteristics present in cable insulation, cable joints and termination failures based on 63 occurrences. Reference [8] identifies three characteristics: short bursts; wavelet coefficients; and arcing. It presents a good and original analysis on this subject. No satisfactory conclusion regarding cable failures is drawn due to the need for more data. Short duration impulses are reported as occurring predominantly on cable terminations. Finally, arcing characteristics for the various failure types are presented. There is a difference in the probability of arcing voltage between the several failures types.

The present paper aims at presenting a research on underground cable network failure waveform based on a high number of failure waveforms (206), more waveform characteristics and comprising more and different failure types, as compared to [8]. Thus, this paper brings an increased knowledge on this particularly important subject. This paper presents original work, not often available in the literature, and the authors hope it will provide valuable insight for both research and utility engineers.

2. Failure Waveform Data

Obtaining fault waveform of distribution system faults has been made easier in recent years due to the increasing presence of digital protection systems. Today's protection systems can record the waveforms of the power system disturbances and make them available in the standard COMTRADE format. Modern protection units can store around 100 disturbance records while older ones would store less than 10. There are also disturbance records automatic retrieval systems that can download the COMTRADE files from the protection unit and upload them to a central repository. Sampling frequencies of protection units are usually in the 800 Hz to 2000 Hz range (for a 50 Hz system).

In addition to a greater percentage of digital relays in the network, utilities have been installing power quality monitoring devices. These devices are also able to record distribution system fault waveforms if correctly set. However, they are mostly intended to observe voltages (as all power quality standards refer to voltages) and have a limited number of inputs for currents. As a result, not all currents are observed. Power system monitoring devices usually present sampling frequencies of 128 or 256 samples/cycle (corresponding to 6.4 kHz or 12.8 kHz for a 50 Hz system; 7.68 kHz or 15.36 kHz for a 60 Hz

system). The latest generation of protection units is starting to show similar sampling frequencies to those of power quality monitoring devices.

A large number (206) of disturbance records from the underground Portuguese distribution network was obtained by using the EDP Distribuição infrastructure. These records correspond to a seven-year period, between 2009 and 2016. The failures were classified according to the following types:

- cable insulation failure (115 events);
- cable joint failure (56 events);
- excavation-caused failure (19 events);
- secondary substation busbar failure (16 events).

For each failure type, there is a large number of records.

3. Failure Waveform Characteristics

3.1. Fault Type

One of the most obvious characteristics of a fault is the number of affected phases. This is referred to as fault type in this paper and can have four options: phase-to-ground; phase-to-phase; phase-to-phase-to-ground; three-phase.

In a mainly triple single-core-cable network, it is expected that the faults are mainly phase-to-ground. However, other types of failures not directly related to cable ageing can present a different type of faults. Some faults may evolve over a short period of time from one type to another (e.g., phase-to-ground to phase-to-phase-to-ground). In this analysis the fault type presented is the last fault type detected.

Signal processing for determining the appropriate fault type from raw data has been addressed in [9,10]. However, both methods presented in [9,10] are not resilient to simple connection errors (e.g., switching phase B with C). These connection errors do not influence the feeder's protection but do influence the faulty phase selection. So, the option in this paper is to use a method of threshold violation by phase. The threshold was set considering the characteristics of the underground network's neutral current limiting impedance. Fault types were classified according to the faulty phases in the instant before the fault clears by circuit breaker action. The fault types for the network's failures waveform data are presented in Table 1.

Table 1. Fault type of the observed failures.

Failure Type	Phase-to-Ground	Others
Cable insulation	111 (97%)	4 (3%)
Excavations	18 (95%)	1 (5%)
Secondary substation	3 (19%)	13 (81%)
Cable joint	45 (80%)	11 (20%)

As expected, the percentage of phase-to-ground faults in cable insulation failures is above 95%. Excavations do seem to involve only one phase in 95% of the cases, which is curious since a large number is due to large-size excavators which one could expect to affect more than one phase. In secondary substation busbar failures, most faults (~80%) involve at least two phases which is probably due to the small insulation distances within a secondary substation busbar. Finally, around 80% of joint failures originated phase-to-ground failures.

3.2. Evolving Faults

Some faults may start as being of a certain type and, as time passes, can encompass other phases or the ground.

Usually, the fault starts out as only affecting a phase and then ends up affecting more phases. Some types of failures may be more prone to evolving faults than others and therefore, it is beneficial to distinguish these faults from others, and so we present data regarding this characteristic.

Identifying evolving faults is relatively simple once there is a fault type identification algorithm. It is enough to determine the fault type over the various time instants in which the fault was sustained to determine if a change occurred. Evolving faults can only apply to faults which affect more than one phase, because the fault type, in this paper, is determined as being the final type of the fault. Observations of evolving faults for the various types of failures are shown in Table 2.

In Table 1, the faults are classified by the number of faulty phases in the instants before the fault clears by circuit breaker action. Therefore, if a fault affects only one phase from the beginning to the end, there is no benefit in being considered as shown in Table 2. Table 2 only displays the 29 faults that affect more than one phase (classified as "others" in Table 1).
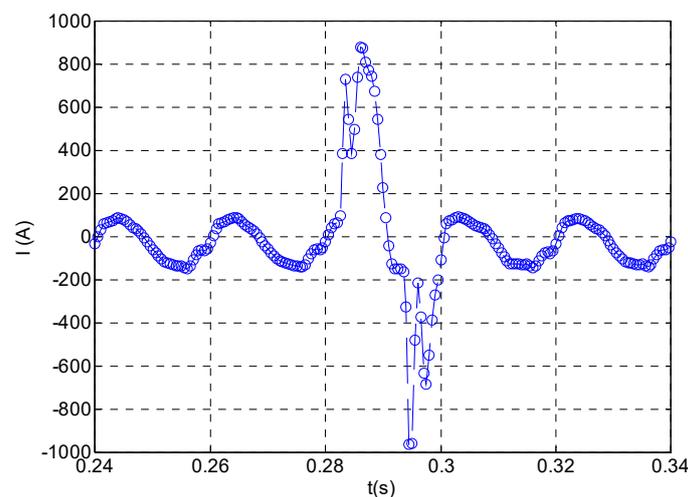
Table 2. Fault type of the observed failures.

Failure Type	Evolving	Not Evolving
Cable insulation	3	1
Excavations	0	1
Secondary substation	8	5
Cable joint	9	2

As shown in Table 2, when a fault affects more than one phase, it is usually the result of an evolving fault, which typically starts out as phase-to-ground fault. This conclusion is irrespectively of the failure type.

3.3. Self-Extinct Faults

Self-extinct faults are faults that are cleared by themselves. During the analysis, self-extinguished faults were observed for some types of failures and for some events. The occurrence of this type of fault always led to a permanent fault within a few seconds, for the cases analyzed in this paper. Incipient faults have been addressed in literature such as [11]. Figure 1 shows the fault current waveform of a self-extinct real fault.

Figure 1. Real case of a self-extinct fault in a 10 kV underground distribution system.

Fault self-extinction in an underground cable network does seem unlikely, from a theoretical point of view, because the known conditions that favor this phenomenon do not apply.
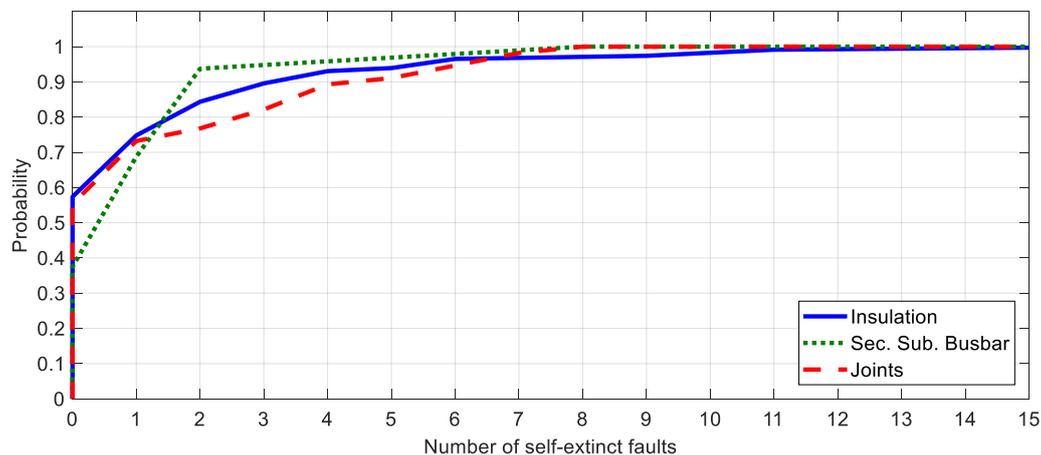
Usually, fault self-extinction is related to a small fault current and small transient voltage in the faulty phase [12]. These conditions are present when using a Petersen coil for the distribution system neutral grounding. However, it is unusual for an underground distribution system to have such a limiting phase-to-ground fault current arrangement due

to the need for increased levels of network insulation and a higher sizing of the Petersen coil, which needs to compensate a large capacitive current.

In Portugal, the option taken for neutral grounding is low impedance grounding with a reactance that limits ground fault currents up to 1000 A. Even under these conditions, the self-extinction phenomenon has been observed.

Detecting a self-extinct fault is also relatively simple by observing that the power system changed from a fault state to a normal load state (existence of load current). Distinguishing between normal load current and circuit breaker opening is performed by detecting a zero-current condition on the feeder after the fault disappears. Zero current is caused by circuit breaker opening and is easy to detect in a fault current waveform.

The number of self-extinguished faults in the minutes prior to the permanent failure was assessed for the available data and the results are presented in Figure 2. The available data shows that around 45% of cable insulation and cable joint failures present previously self-extinct faults while the percentage is around 60% for secondary substation busbar failures. For this type of failure, the number of self-extinct faults prior to the permanent fault is lower when compared to the remaining failure types. In none of the excavation-caused failure data were self-extinct faults observed.

Figure 2. Observed cumulative probability for the number of self-extinct faults.
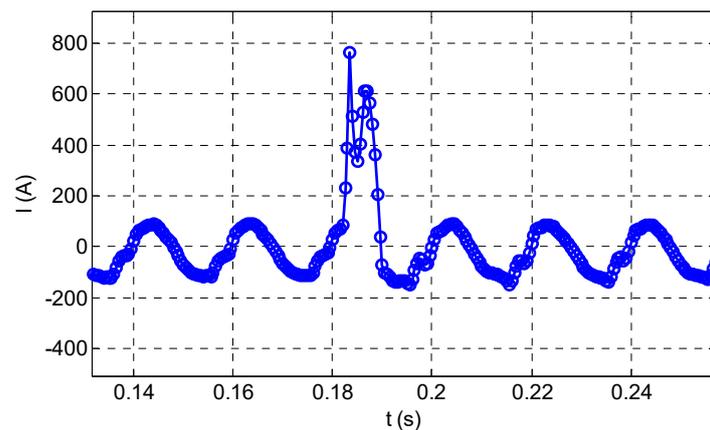
Self-extinct faults numbering above eight have only been observed for cable insulation failures.

It is possible that some self-extinct faults may not have been recorded, for some failure events, due to the disturbance recording settings or limitations of the protection unit. Therefore, the real percentage of failures displaying self-extinct faults prior to the permanent failure may be higher.

3.4. Sub-Cycle Self-Extinct Faults

Sub-cycle self-extinct faults are very similar to self-extinct faults with the key difference that between the fault inception instant and the fault clearing instant, less than one power system period (20 ms for 50 Hz networks and 16.7 ms for 60 Hz networks) has passed. Their duration is smaller than a power system cycle.

An option was made to consider these type of faults separately from other self-extinct faults to check if the data presents differences regarding multi-cycle self-extinct faults. Figure 3 shows a real example of a sub-cycle self-extinct fault in a 10 kV network.

Figure 3. Real case of a sub-cycle self-extinct fault in a 10 kV underground distribution system.

This fault lasts for about half a cycle until it is cleared when the fault current passes by zero.

Detection of a sub-cycle fault may be carried out by using the premise that to occur, there must not be a multiple cycle fault within the observed period. The algorithm used by the authors identifies the samples in the current that present a large difference relative to the expected value had there been no fault. The expected value is determined by calculating the Fourier transform of the previous cycle of the fault current and estimating the next sample's value.

$$\hat{x}_i = \frac{1}{N}\left|\overline{X}_{1h}\right|cos\left(\frac{2\pi}{N} + arg\left(\overline{X}_{1h}\right)\right) \tag{1}$$

In (1), $\hat{x}_i$ refers to the estimated value for the sample, $\overline{X}_{1h}$ is the complex Fourier coefficient for the first harmonic calculated with the samples of the previous cycle, N is the number of samples per cycle and $arg()$ is a function that determines the angle of a complex number.

If (2) holds then there is a high probability of being a sub-cycle fault.

$$|x_i - \hat{x}_i| > kx_{max} \tag{2}$$

In (2), x_i is the sample under evaluation, x_{max} is the maximum absolute value of the current in the previous cycle and k is a threshold; a value of $k = 0.05$ was used.
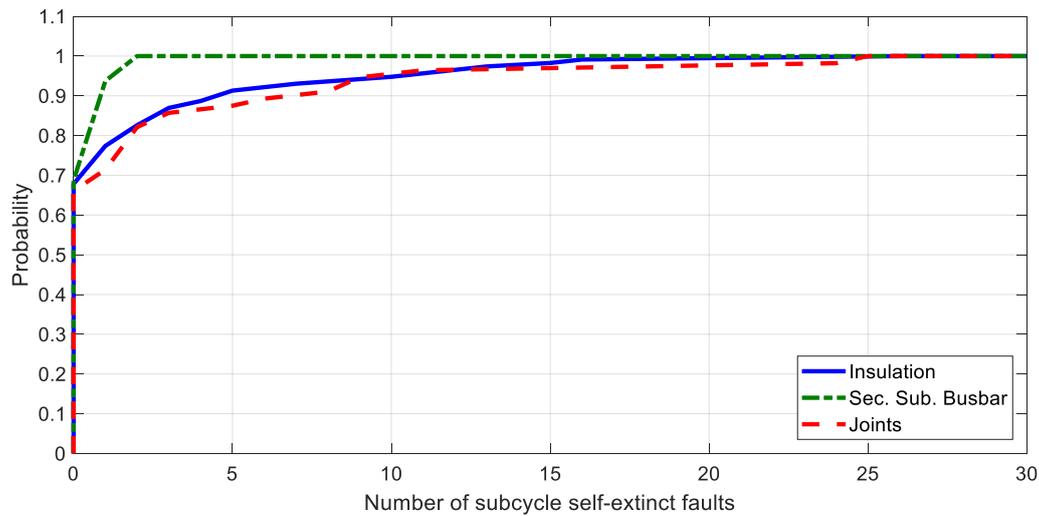
There is one more condition that must hold which is that Condition (2) must hold for at least a few consecutive samples (in this paper we considered three consecutive samples). If Condition (2) holds for more than N samples, then it lasts for more than one cycle and, therefore, it is not a sub-cycle fault and is discarded.

The algorithm for sub-cycle self-extinct fault was applied by the authors to the dataset of failure waveforms. The results are presented in Figure 4.

Consistently with the results presented in Section 3.3, no sub-cycle self-extinct fault occurred for excavation-motivated failures. This result is expected because this type of failure is caused by an external action and not ageing. Moreover, if a fault does not display sub-cycle self-extinct, the probability of being an excavation-caused failure is high.

The number of sub-cycle self-extinct faults before a secondary substation busbar failure is low when compared with the remaining failure types.

Both cable insulation and joint failures present nearly overlapping curves in Figure 4. When comparing with multi-cycle self-extinct faults (Figure 2), there was a slight difference in the cumulative distribution data for cable insulation and joint failures.

Figure 4. Observed cumulative probability for the number of sub-cycle self-extinct faults.

Overall, only 30% of insulation, joints and secondary substation busbar failures presented sub-cycle faults. However, one may not exclude the possibility that some protection units did not record these events due to the disturbance recording settings or other limitations.

3.5. Fault Inception Instant

Voltages in AC power systems have a sinusoidal shape, therefore, at certain instants of time, they reach their absolute maximum and at other time instants, they pass by zero. So, there is a wide range of voltage values between the maximum absolute value and zero for a failure to occur. The question this section seeks to answer is if the value of instantaneous voltage at the instant where the fault occurred can provide information regarding the failure type. For that purpose, the instantaneous voltage at the fault inception instant relative to the absolute maximum needs to be determined.

Fortunately, a fault inception is always an abrupt event for the voltages and currents of the power system. There are several algorithms to detect abrupt event changes based on statistical signal analysis [13–16]. However, the authors found that for faults that do not originate an extremely abrupt behavior (e.g., fault inception near zero instantaneous voltage or high fault resistances), these algorithms sometimes fail to detect the abrupt event.

Therefore, another method, based on [17], was developed by the authors and then applied to the failure waveform data. The method consists of determining if two sequential voltage cycles do not present a similar RMS value.

$$\sqrt{\frac{1}{N}\sum_{k=i+1}^{i+N} x_k^2} < (1-R)\sqrt{\frac{1}{N}\sum_{k=i-N}^{i-1} x_k^2} + S \tag{3}$$

In (3), i is the sample being tested, R is an error margin depending on the value (a 5% value was used) and S is a minimum value of a change to have occurred (0.01 Vmax was used).

If (3) holds then there must be an abrupt change somewhere within the cycle after sample i. The next step is to identify the sample for which the abrupt change occurs.

A cycle length window before sample i (designated as state $S1$) is used to determine the Fourier transform up to the 5th harmonic (if the signal's sampling frequency is enough). An identical process is used for the cycle immediately after sample i (designated as state

*S*2). Then x_i is estimated considering the Fourier transform of the signal in the previous cycle (*S*1) and considering the Fourier transform of the signal in the next cycle (*S*2).

$$(\hat{x}_i)_{S1} = \frac{1}{N} \sum_{h=1}^{3} \left| \overline{X}_{2h-1}^{S1} \right| cos\left(2\pi(2h-1)\frac{1}{N} + arg\left(\overline{X}_{2h-1}^{S1} \right) \right) \tag{4}$$

$$(\hat{x}_i)_{S2} = \frac{1}{N} \sum_{h=1}^{3} \left| \overline{X}_{2h-1}^{S2} \right| cos\left(2\pi(2h-1) + arg\left(\overline{X}_{2h-1}^{S2} \right) \right) \tag{5}$$
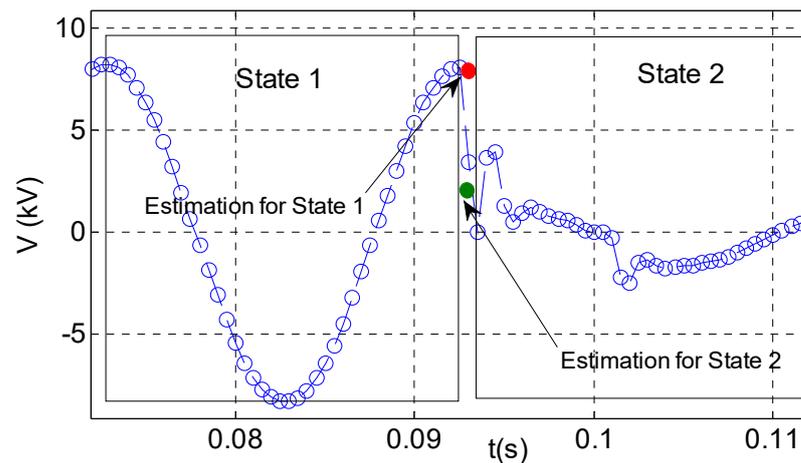
where, h is the number of the harmonic and $\overline{X}_{2h-1}^{S1}$ is the complex Fourier coefficient for state 1.

Both estimates, from (4) and (5), are then compared with the actual sample value. If an abrupt change has occurred at that sample then the distance between the sample and the result of (5) will be smaller than the distance between the sample and the result of (4), i.e., if Condition (6) holds.

$$|(\hat{x}_i)_{S1} - x_i| > |(\hat{x}_i)_{S2} - x_i| \tag{6}$$

where, $(\hat{x}_i)_{S1}$ is the estimated sample under the assumption that the system is on state 1 and $(\hat{x}_i)_{S2}$ is the estimated sample under the assumption that the system is on state 2.
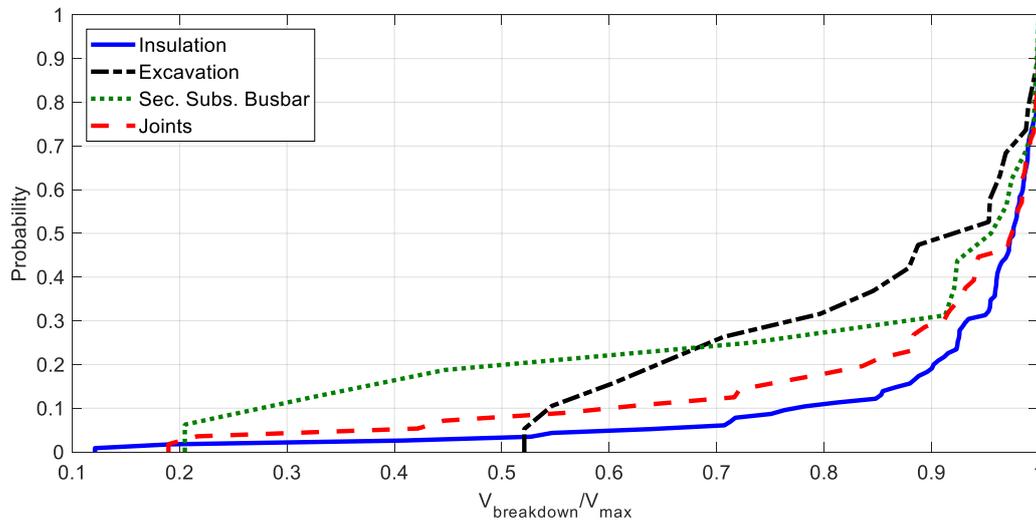
The process can be seen graphically in Figure 5.

Figure 5. Example of the algorithm for determining abrupt changes in the waveform. There are two estimates for the suspected sample at which the abrupt change could have occurred (sample *i*): one comprising the previous cycle's sampling set; the second comprising the next cycle sampling set. If the distance between the observed sample *i* and the estimate of sample *i* using the state 2's sampling set (next cycle's samples) is smaller than the distance between the observed sample *i* and the estimate of sample *i* using state 1's sampling set (previous cycle samples), then an abrupt change has occurred.

When working with sampled signals, the precise time instant when the abrupt fault occurred is never known. The best information available is that at instant $i - 1$, there was no fault and that at instant i there is a fault. So, the fault occurred between instants $i - 1$ and i but the information regarding the actual instant is not known. The authors considered that fault instant follows a uniform distribution between $i - 1$ and i. To minimize the error related to sampling frequency, the authors considered the abrupt change occurred at $i - 1/2$ and the voltage is estimated, based on state *S*1, for this time instant.

The authors applied the algorithm described above for the entire set of the 206 failure waveform records. Results are shown in the form of cumulative probability in Figure 6.

The observations show that if the instantaneous voltage, at which the fault occurs, is near its maximum, the probability of a cable insulation failure is the highest. Joint failures have a slightly higher probability of occurring when the voltage is not nearer to

the maximum. The observations for these two types of failures were expected because they are both caused by insulation ageing processes.

Figure 6. Observed cumulative probability for the voltage at the fault inception instant.

Excavations present a higher probability of occurring with lower voltages which is consistent with their nature as an external aggression on the insulation.

Finally, the available data show that the secondary substation busbar failures present a higher probability of occurring for low voltages than insulation and joints but increases very slowly until 0.9 where its behavior is similar to that of joint failures.

3.6. Electric Arc

Electric arcs are common when faults occur. They present several interesting characteristics which are worthwhile to determine if they are used to distinguish between several types of failures.

One of the most interesting characteristics is to detect the presence of an electric arc. Another one is the electric arc length, which is proportional to the arc voltage [18–20]. Therefore, it can be used to determine if the arc has formed between insulation with a higher length (e.g., outdoor insulators) or smaller lengths (e.g., cables).

However, electric arcs are non-linear; in fact, the electric arc voltage is more similar to a square curve [18]. Therefore, it is not possible to determine that arc's characteristics in the power system frequency domain. Time domain equations must be used [20]. The equation used to model the electric arc [20], is given by:

$$v_s \simeq Ri_s + L\frac{di_s}{dt} + V_a sgn(i_{arc}) \tag{7}$$

In (7), v_s is the source voltage (voltage in substation busbar), R is the resistance up to the point where the arc has formed, i_s is the current supplied by the source (current at the feeder), L is the inductance of the lines and cables up to the point where the arc has formed, V_a is the arc voltage, i_{arc} is the current flowing through the electric arc and *sgn* is the sign function which is 1 if the input number is positive and -1 if the input number is negative.

For single point neutral grounded systems, such as the Portuguese, the current flowing through the arc can be approximated by the zero-sequence current, for phase-to-ground faults.

The problem is now to determine R, L and V_a in (7). There is only one equation to determine the three variables, however, there is a sufficiently high number of samples to accomplish this. Then, the problem is fitting the data to the model of (7) which is achieved by using (8).

$$\min_y \|Ay - v_2^2\| \; where \; y_i \geq 0 \tag{8}$$

In (8), $y = [R \; L \; V_a]^T$, v is a vector with all samples (N) of the source voltage for the considered time period and A is a $N \times 3$ matrix presented in (9).
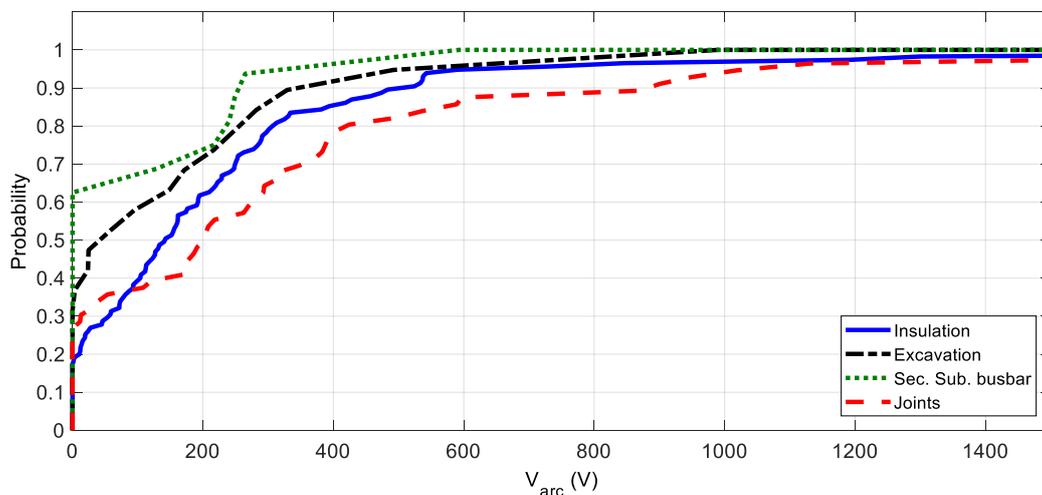
$$A_{N \times 3} = \begin{bmatrix} i_{s_i} & \frac{i_{s_{i+1}} - i_{s_{i-1}}}{t_{i+1} - t_{i-1}} & sgn\left(i_{0_i}\right) \\ i_{s_{i+1}} & \frac{i_{s_{i+2}} - i_{s_i}}{t_{i+2} - t_i} & sgn\left(i_{0_{i+1}}\right) \\ i_{s_{i+2}} & \frac{i_{s_{i+3}} - i_{s_{i+1}}}{t_{i+3} - t_{i+1}} & sgn\left(i_{0_{i+2}}\right) \\ \vdots & \vdots & \vdots \end{bmatrix} \quad (9)$$

where, i_{s_i} refers to sample i of the current at the feeder point, t_i is the time at which sample i was recorded, i_{0_i} refers to the sample i of the zero-sequence current measured at the feeder point.

However, (8) cannot be solved with a standard least-squares method because none of the variables in vector y can be negative. There is no physical meaning to any of the variables of vector y with negative values [20]. The solution of (8) can be obtained by using the method described in chapter 23 of [21] which is implemented in the MATLAB optimization toolbox as a nonnegative least-squares constraints problem solver.

Arc voltage is calculated for each fault cycle which leads to a set of values for the arc voltage; electric arcs are notorious for not being constant. For this purpose, the authors considered the median value of the electric arc voltages obtained for each half-cycle of the fault.

The authors applied the arc voltage algorithm to the set of failure waveforms. The results are presented in Figure 7.

Figure 7. Observed cumulative probability for the arc voltage.

The available data shows that cable joint failures present the higher arc voltages, which may be due to their internal design and materials. Next, cable insulation failures are the ones for which the arc voltage is the second highest. This was expected because the insulation distance in a cable is smaller than that of a joint.

Excavation-caused failures present lower electric arc voltages—which can be explained as being the result of an external aggression which causes the cable sheath to be in close range of the core. Therefore, the distance between these two is smaller than in normal conditions (set by the cable insulation failure).

Secondary substation busbar failures present the smallest arc voltages probably because of the small insulation distances and the higher fault currents. This type of failure usually leads to a phase-to-phase fault which present higher fault currents. The arc voltage is inversely proportional to the arc current [18].

3.7. Intra-Cycle Fault Self-Extinction

Intra-cycle fault self-extinction phenomenon is probably the most unusual and the one most readers will be unfamiliar with.

Electric arc self-extinction depends on the value of the current [22]. However, in a sinusoidal system, the current will cross zero every half-cycle. At those points, the arc can experience a temporary extinction because the arc voltage is small as well as the current. When the fault extinguishes, the faulty phase voltage will return to pre-fault values causing the fault, and electric arc, to re-appear. This process can repeat itself for every half-cycle. Figure 8 shows a real case of an intra-cycle fault self-extinction in a 10 kV network. Notice that every time the current crosses zero, the next samples of current are smaller than expected and the faulty phase voltage presents an abrupt change with higher values.

The real example of Figure 8 was recorded in a 1000 A neutral grounding low impedance network. Other types of neutral grounding arrangements may lead to other waveforms.
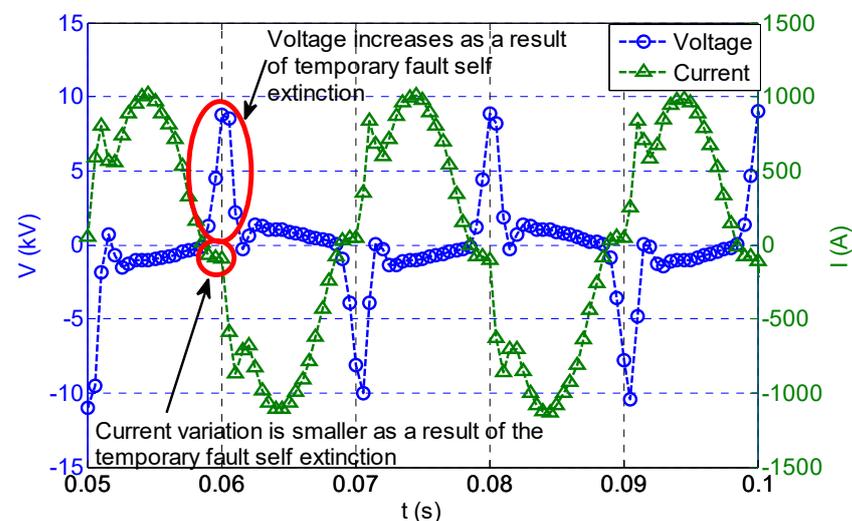

Figure 8. Observed cumulative probability for the arc voltage.

Detection of time instant when this event occurred is necessary. However, self-extinction can be accompanied with charge/discharge transients of the network's distributed capacities which will be observed in the voltage and in the current [23], depending on the neutral grounding arrangement. The authors developed an algorithm for the detection of intra-cycle self-extinct faults; however, it may not hold for networks with neutral grounding arrangements other than single point low impedance.

Firstly, the algorithm checks if the fault current has passed by zero. If it is true, it then checks if the next samples present value differences similar to those observed when the fault was present. If the fault current is near zero or difference between samples is small, then the fault has temporarily self-extinguished.

Secondly, the differences between consecutive voltage samples are checked for larger than expected variations in a normal sinusoidal wave using (10).
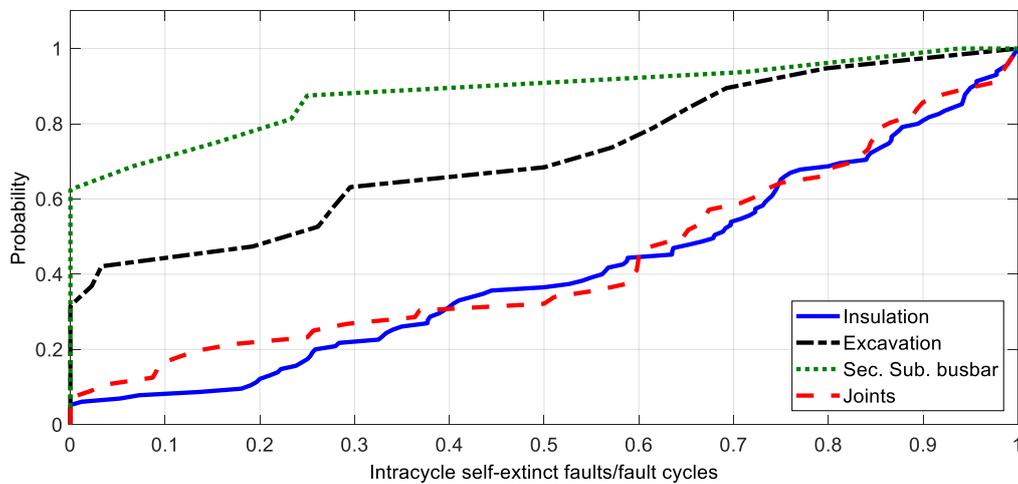
$$|\Delta v| = |v_i - v_{i-1}| \leq V_{max} \frac{2\pi}{N} \tag{10}$$

where, v_i is the sample I of the voltage and V_{max} is the maximum of the sinusoidal wave.

If (10) does not hold at some sample after the fault current zero crossing, then a fault self-extinction and re-establishment has been detected.

This algorithm was applied by the authors to the failure waveform data. There are at least two types of information that can be retrieved from this phenomenon: the percentage of intra-cycle self-extinct faults with relation to the number of half-cycles in the fault; and

the voltage that caused the insulation breakdown. The cumulative probability of the first feature is presented in Figure 9.
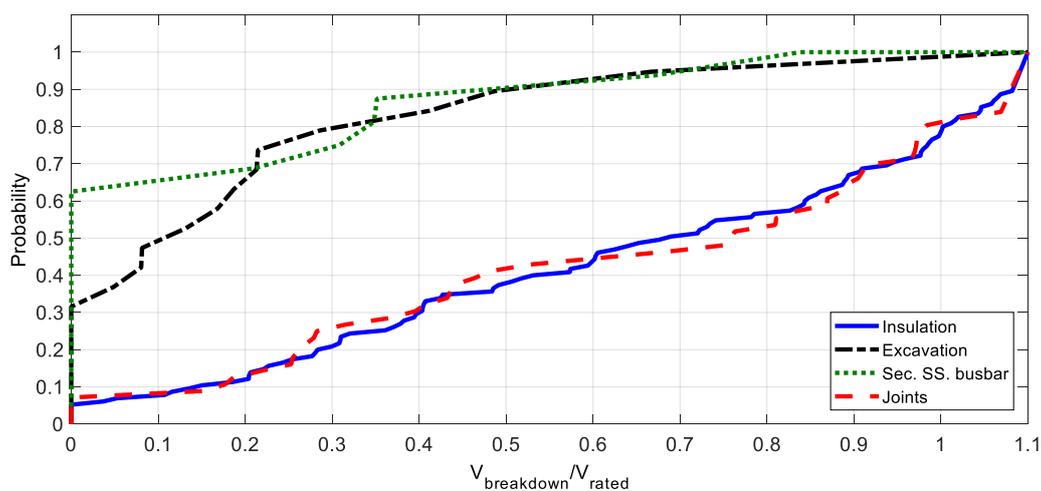

Figure 9. Observed cumulative probability for intra-cycle self-extinct fault cycles' relation to the total number of fault cycles.

The failures which present a higher probability of intra-cycle self-extinct faults are cable insulation and joint. Their curves are very similar. Intra-cycle self-extinct faults are probably caused by solid insulation ageing processes which are due to ageing.

Next, excavation-motivated failures present typically a smaller number of intra-cycle self-extinct faults and in 30% of cases, none at all. As previously stated, this type of failure is not caused by ageing and therefore it is less likely to present intra-cycle self-extinct faults.

Finally, secondary substation busbar failures typically originate multi-phase faults which have been found not to present intra-cycle self-extinct faults. This type of fault has only been detected in phase-to-ground faults.

There is another type of information that can be retrieved from intra-cycle self-extinct faults which is the voltage at which the fault reappears. The results for this are presented in Figure 10.

Figure 10. Observed cumulative probability for intra-cycle self-extinct fault breakdown voltage.

A close similarity between the results for cable insulation and joint are also present in Figure 10, which means that intra-cycle self-extinguished faults manifest themselves in the same manner for these types of failures. Curiously, the breakdown voltage can be very small, as 50% of self-extinct faults occur at less than 40% of rated voltage. This value is

90% for the remaining two types of failures which means that phase-to-ground insulation intermittent breakdown is not a characteristic of these type of failures.

4. Conclusions

This paper shows an investigation on the waveform characteristics of faults caused by four types of failures in MV cable networks. About 200 real failure waveforms from the Portuguese MV underground network were analyzed.

Seven characteristics extracted from failure waveform data were identified: fault type (e.g.,: phase-to-ground); evolving fault; self-extinct fault; sub-cycle self-extinct fault; fault inception instant; arc voltage; and intra-cycle fault self-extinction. Each of these characteristics was extracted from the available failure waveform data. The probability for each of the characteristics to ascertain any of the four failure types was estimated and shown by a cumulative probability graph.

The data analysis shows that secondary substation busbar failure faults typically involve more than one phase, while the other remaining failures originate mainly phase-to-ground faults. Fault self-extinction, either sub-cycle or multi-cycle, has not been observed in excavation-caused failures. Cable insulation and cable joint failures display similar probabilities for sub-cycle and multi-cycle self-extinct faults. Fault self-extinction was observed for secondary substation busbar failures but in low numbers, i.e., the maximum number of self-extinct faults was 2 while it reached 20 for the remaining failure types.

Different results for each failure type were observed for fault inception instant and arc voltage. These characteristics have shown to be the most promising for distinguishing between failure types.

Finally, the data shows that intra-cycle self-extinction for excavation-caused failures and secondary substation busbar failures is different when compared with the remaining failure types. This is advantageous for a failure identification process. However, intra-cycle self-extinction in cable insulation and joint failures was found to be similar.

References

1. Kulkarni, S.; Santoso, S. Time-Domain Algorithm for Locating Evolving Faults. *IEEE Trans. Smart Grid* **2012**, *3*, 1584–1593. [CrossRef]
2. Kulkarni, S.; Santoso, S.; Short, T.A. Incipient Fault Location Algorithm for Underground Cables. *IEEE Trans. Smart Grid* **2014**, *5*, 1165–1174. [CrossRef]
3. Zimmerman, K.; Costello, D. Impedance-Based Fault Location Experience. In Proceedings of the 2006 IEEE Rural Electric Power Conference, Albuquerque, NM, USA, 9–11 April 2006.
4. Krishnathevar, R.; Ngu, E.E. Generalized Impedance-Based Fault Location for Distribution Systems. *IEEE Trans. Power Deliv.* **2012**, *27*, 449–451. [CrossRef]
5. Sachdev, M.S.; Agarwal, R. A technique for estimating transmission line fault locations from digital impedance relay measurements. *IEEE Trans. Power Deliv.* **1988**, *3*, 121–129. [CrossRef]
6. Nakamura, H.; Mizuno, Y. Method for Diagnosing a Short-Circuit Fault in the Stator Winding of a Motor Based on Parameter Identification of Features and a Support Vector Machine. *Energies* **2020**, *13*, 2272. [CrossRef]

7. Yogee, G.S.; Mahela, O.P.; Kansal, K.D.; Khan, B.; Mahla, R.; Alhelou, H.H.H.; Siano, P. An Algorithm for Recognition of Fault Conditions in the Utility Grid with Renewable Energy Penetration. *Energies* **2020**, *13*, 2383. [CrossRef]

8. Kulkarni, S.; Allen, A.J.; Chopra, S.; Santoso, S.; Short, T.A. Waveform characteristics of underground cable failures. In Proceedings of the IEEE PES General Meeting, Minneapolis, MN, USA, 25–29 July 2010.

9. Kasztenny, B.; Campbell, B.; Mazereeuw, J. Phase selection for single-pole tripping weak infeed conditions and cross-country faults. In Proceedings of the 27th Annual Western Protective Relay Conference, Spokane, WA, USA, 24–26 October 2000.

10. Anderson, P.M. *Analysis of Faulted Power Systems*; Wiley-IEEE Press: New York, NY, USA, 1995.

11. Liu, N.; Fan, B.; Xiao, X.; Yang, X. Cable Incipient Fault Identification with a Sparse Autoencoder and a Deep Belief Network. *Energies* **2019**, *12*, 3424. [CrossRef]

12. Willheim, R.; Waters, M. *Neutral Grounding in High-voltage Transmission*; Elsevier Publishing Company: Amsterdam, The Netherlands, 1956.

13. Saha, M.M.; Izykowski, J.J.; Rosolowski, E. *Fault Location on Power Networks*; Springer: London, UK, 2009.

14. Gilbert, D.M.; Morrison, I.F. A statistical method for detection of power system faults. In Proceedings of the International Conference on Power System Transients, Lisbon, Portugal, 3–7 September 1995.

15. Ukil, A. Application of Abrupt Change Detection in Power Systems Disturbance Analysis and Relay Performance Monitoring. *IEEE Trans. Power Deliv.* **2007**, *22*, 59–66. [CrossRef]

16. Kwon, W.H.; Lee, G.W.; Park, Y.M.; Yoon, M.C.; Yoo, M.H. High impedance fault detection utilizing incremental variance of normalized even order harmonic power. *IEEE Trans. Power Deliv.* **1991**, *6*, 557–564. [CrossRef]

17. Basseville, M.; Nikiforov, I.V. *Detection of Abrupt Changes: Theory and Application*; Prentice Hall: Englewood Cliffs, NJ, USA, 1993.

18. Terzija, V.V.; Koglin, H.J. On the modeling of long arc in still air and arc resistance calculation. *IEEE Trans. Power Deliv.* **2004**, *19*, 1012–1017. [CrossRef]

19. Russell, B.; Chinchali, R. A digital signal processing algorithm for detecting arcing faults on power distribution feeders. *IEEE Trans. Power Deliv.* **1989**, *4*, 132–140. [CrossRef]

20. Djurić, M.B.; Radojević, Z.M.; Terzija, V.V. Time domain solution of fault distance estimation and arcing faults detection on overhead lines. *IEEE Trans. Power Deliv.* **1999**, *14*, 60–67. [CrossRef]

21. Lawson, C.L.; Hanson, R.J. *Solving Least Squares Problems*; Society for Industrial and Applied Mathematics: Philadelphia, PA, USA, 1987.

22. Basler Technical Papers. Automatic Reclosing—Transmission Line Applications and Considerations. Available online: www.basler.com (accessed on 13 June 2018).

23. Druml, G.; Kugi, A.; Seifert, O. A new directional transient relay for high ohmic earth faults. In Proceedings of the CIRED 2003—17th International Conference and Exhibition on Electricity Distribution, Barcelona, Spain, 12–15 May 2003.